

Leveling cartoons, texture energy markers, and image decomposition

PETROS MARAGOS and GEORGIOS EVANGELOPOULOS

*School of Electrical and Computer Engineering, National Technical University of
Athens, Greece*

{maragos,gevag}@cs.ntua.gr

Abstract The variational $u + v$ model for image decomposition aims at separating the image into a ‘cartoon component’ u , which consists of relatively flat plateaus for the object regions surrounded by abrupt edges, and a ‘texture component’ v , which contains smaller-scale oscillations plus possibly noise. Exploiting this model leads to improved performance in several image analysis and computer vision problems. In this paper we propose alternative approaches for $u + v$ decomposition based on levelings and texture energy. First, we propose an efficient method for obtaining a multiscale cartoon component using hierarchies of levelings based on Gaussian scale-space markers. We show that this corresponds to a constrained minimization driven by PDEs and link the leveling cartoons with total variation minimization. Second, we extract the texture component from levelings of the residuals between the image and its multiscale levelings. Further, we employ instantaneous nonlinear operators to estimate the spatial modulation energy in the most active texture frequency bands and use this as a new type of texture markers that yield an improved texture component from the leveling residuals. Finally, we provide experimental results that demonstrate the efficacy of the proposed image decomposition methods.

Keywords: leveling, texture, energy, image decomposition.

1. Introduction

Decomposing an image f into its structural part (objects or geometric features at various scales represented by their regions, boundaries, and mean intensities) and its texture part is both an interesting problem as well as an approach useful for many image analysis and vision applications, such as enhancement, inpainting, segmentation, texture and shape analysis, object description.

A recently proposed method for image decomposition is the $f = u + v$ model, where the u part is called the ‘cartoon component’ and consists of relatively smooth or flat plateaus for the object regions surrounded by abrupt intensity walls, whereas the small-amplitude oscillatory v part is called the ‘texture’. If there is also noise or some other type of insignificant

residual w , then a refined model $f = u + v + w$ may be used. Next we summarize some previous works in this area and outline our new contributions.

Background on image decomposition: Many of the nonlinear edge-preserving image smoothing schemes can create cartoon approximations of an image. Examples include the anisotropic diffusion and image selective smoothing. Several of these schemes have been shown in [11] to be special cases or closely related to the Mumford-Shah energy functional [12]

$$E_{MS}(u, C) = \iint_{R \setminus C} (|\nabla u|^2 + \lambda(u - u_0)^2) dx dy + \mu \text{Len}(C). \quad (1)$$

Actually, one way of obtaining a piecewise-smooth cartoon u from an initial image u_0 is via minimization of the above functional by searching for those u that are *piecewise-constant* on the regions R . This has been used both for denoising and boundary detection. Another approach is via the total variation (TV) image denoising method [14] which finds a cartoon u by minimizing the TV norm $\iint_R |\nabla u|$ subject to $\iint_R (u - u_0) = 0$ and $\iint_R (u - u_0)^2 = \sigma^2$, or equivalently by minimizing the functional

$$E_{ROF}(u) = \iint_R |\nabla u| dx dy + \lambda \iint_R (u - u_0)^2 dx dy, \quad (2)$$

on some image domain R . This minimization is done via a PDE (gradient-descent) solver that finds a local minimum of the TV functional. While the TV approach performs well for edge-preserving image denoising, it may not preserve texture for small λ . Y. Meyer [10] changed the TV optimization problem (2) by using instead of the L_2 norm other norms that are more appropriate to preserve texture. Thus, Meyer introduced the decomposition of an image f into a model $u + v = f$ where u and v result from the modified optimization problem, u is some type of cartoon while v contains the texture (plus possibly noise).

Vese & Osher [16, 17] developed a PDE-based iterative numerical algorithm to estimate the u and v components by approximating Meyer's weaker norms. Texture is assumed to be an oscillating function

$$v = \text{div}(\vec{g}) = \partial_x g_1 + \partial_y g_2, \quad (3)$$

where the vector \vec{g} captures variation in the vertical and horizontal image directions. The component v may exhibit large oscillations, but yields a small metric as measured by the norms $\|\vec{g}\|_{L^p} = (\iint |\vec{g}|^p)^{1/p}$. For $p \rightarrow \infty$, norm L^p approximates L^∞ and thus the norm of Meyer's space of oscillating functions [10]. A three-component $f = u + v + w$ decomposition model was formulated with the (u, v) components derived by minimizing

$$E_{VO}(u, \vec{g}) = \iint_R |\nabla u| dx dy + \lambda \iint_R |f - (u + \text{div}(\vec{g}))|^2 dx dy + \mu \|\vec{g}\|_{L^p}, \quad (4)$$

and the residual $f - u - v$ giving image noise w . By letting $\lambda, p \rightarrow \infty$, this scheme approximates the initial decomposition proposed by Meyer.

The above ideas and algorithms for $u + v$ image decomposition have been used for improving image restoration [16] and image inpainting by simultaneous filling-in texture and structure in missing image parts [1].

New contributions: Some open research areas in this interesting $u + v$ decomposition space are: (i) Alternative schemes for estimation of a cartoon u and/or texture v component. (ii) Analysis of the information in the u and/or v components. (iii) Exploitation of this decomposition for improving performance in several image analysis and computer vision problems. In this paper we contribute advances in the first two directions inspired by and further utilizing the $u + v$ idea. First, we propose an efficient method for obtaining a cartoon component, possibly at multiple scales, using nonlinear object-oriented smoothing of the leveling type that is driven by PDEs with global scale-space markers obtained from Gaussian diffusion of the image. We also show optimality of this method via a nonlinear constrained minimization. The residuals among consecutive scales of this leveling pyramid provide us with the texture component. Second, we analyze textural information by using instantaneous nonlinear energy-tracking operators that estimate the spatial modulation energy. This energy tracking focuses on the most active texture frequency bands. Third, we propose an alternative new type of markers for the levelings extracting the texture part which are based on texture modulation energy. Finally, we provide experimental results that demonstrate the efficacy of the proposed methods for $u + v$ decomposition.

2. Levelings: Variational problems

Proofs of the following variational formulations can be found in Maragos [7].

Let $u_0(x, y)$ some smooth initial image and $u(x, y, t)$ some scale-space analysis over some compact image domain R with $u(x, y, 0) = u_0(x, y)$. Maximizing the volume functional by keeping invariant the global supremum

$$\max \iint_R u \, dx dy \quad \text{s.t.} \quad \bigvee u = \bigvee u_0, \quad (5)$$

has a gradient flow governed by the PDE generating flat dilation by disks:

$$u_t = \|\nabla u\|, \quad u(x, y, 0) = u_0(x, y). \quad (6)$$

Similarly, minimizing the volume functional by fixing the global infimum

$$\min \iint_R u \, dx dy \quad \text{s.t.} \quad \bigwedge u = \bigwedge u_0, \quad (7)$$

has a gradient flow governed by the isotropic flat erosion PDE:

$$u_t = -\|\nabla u\|, \quad u(x, y, 0) = u_0(x, y). \quad (8)$$

Imagine now creating a new type of cartoon by starting from a *reference* image $f(x, y)$ consisting of several parts and a *marker* image $M = u_0(x, y)$ (initial seed) intersecting some of these parts and by evolving M toward f in a monotone way such that all evolutions $u(x, y, t)$, $t \geq 0$, satisfy the following partial ordering, $\forall x, y \in R$

$$t_1 < t_2 \implies f(x, y) \preceq_f u(x, y, t_2) \preceq_f u(x, y, t_1) \preceq_f u_0(x, y). \quad (9)$$

The partial order $u \preceq_f g$ means that $f \wedge g \leq f \wedge u$ and $f \vee g \geq f \vee u$. Further, if we partition the following regions R^- and R^+ formed by the zero-crossings of $f - u_0$

$$\begin{aligned} R^- &= \{(x, y) : f(x, y) \geq u_0(x, y)\} = \bigsqcup_i R_i^-, \\ R^+ &= \{(x, y) : f(x, y) < u_0(x, y)\} = \bigsqcup_i R_i^+, \end{aligned} \quad (10)$$

into connected subregions, then the evolution of u is done by maintaining all local maxima and local minima of u_0 inside these subregions R_i^- and R_i^+ , respectively:

$$\bigvee_{R_i^-} u = \bigvee_{R_i^-} u_0 \quad \text{and} \quad \bigwedge_{R_i^+} u = \bigwedge_{R_i^+} u_0, \quad R = \left(\bigsqcup_i R_i^-\right) \sqcup \left(\bigsqcup_i R_i^+\right), \quad (11)$$

where \sqcup denotes disjoint union. Since the order constraint $f \preceq_f u \preceq_f u_0$ implies that $|f - u| \leq |f - u_0|$, the above problem is equivalent to the following constrained minimization

$$\min \iint_R |u - f| dx dy \quad \text{s.t.} \quad \bigvee_{R_i^-} u = \bigvee_{R_i^-} u_0, \quad \bigwedge_{R_i^+} u = \bigwedge_{R_i^+} u_0. \quad (12)$$

Theorem 1. *A gradient flow for the problem (12) is given by the PDE*

$$\begin{aligned} \partial u(x, y, t) / \partial t &= -\text{sign}(u - f) \|\nabla u\|, \\ u(x, y, 0) &= u_0(x, y). \end{aligned} \quad (13)$$

The PDE (13) was introduced in [9]. It was studied systematically in [6] where it was proved that it has a steady-state $u_\infty(x) = \lim_{t \rightarrow \infty} u(x, t)$ which is a *leveling* of f with respect to u_0 , denoted by $u_\infty = \Lambda(u_0|f)$.

A leveling g of some image f was defined geometrically in [9] via the property that, the variation of g between any two close neighbor pixels p, q is bracketed by a larger same-sign variation in the reference image f :

$$g(p) > g(q) \implies f(p) \geq g(p) > g(q) \geq f(q). \quad (14)$$

In [6] levelings were defined algebraically as fixed points of triphase operators $\lambda(M|f)$ that switch among three phases, an expansion, a contraction, and the reference f . Further, the leveling of f w.r.t. $M = u_0$ can be obtained as the limit of iterations of λ :

$$u_\infty = \Lambda(M|f) \triangleq \lim_{n \rightarrow \infty} \lambda^n(M|f) \preceq_f \cdots \lambda(M|f) \preceq_f M = u_0. \quad (15)$$

The simplest choice for λ is $\lambda(M|f) = [f \wedge \delta(M)] \vee \varepsilon(M)$, where δ and ε are disk dilations and erosions.

3. Leveling-based multiscale cartoons

Levelings have many interesting scale-space properties [9]. Due to (9) and (14), they preserve the coupling and sense of variation in neighbor image values, which is good for edge preservation. Further, due to (11) the levelings do not create any new regional maxima or minima. Also, they are increasing and idempotent filters. In practice, they can reconstruct whole image objects with exact preservation of their boundaries and edges. In this reconstruction process they simplify the original image by completely eliminating smaller objects inside which the marker cannot fit. The reference image plays the role of a *global constraint*.

Motivated by all their above attractive properties, we propose an alternative method for u, v decomposition of an original image where we *use the leveling as the cartoon approximation*

$$u = \Lambda(M|f), \quad (16)$$

and its residual $r = f - u$ as containing the texture component v . For u , the marker M plays an important role. Its choice gives us a great flexibility for the final leveling and we could define it based on a multiscale analysis. Specifically, given a reference image f , suppose we can produce various markers M_i , $i = 1, 2, 3, \dots$ that are related to some increasing scale parameter i . Then, if we construct the levelings $u_i = \Lambda(M_i|u_{i-1})$, $i = 1, 2, 3, \dots$, with $u_0 = f$ the cartoon images u_i constitute a hierarchy of *multiscale levelings* possessing the causality property that u_j is a leveling of u_i for $j > i$. One way to construct such multiscale leveling cartoons is to use a sequence $M_i = f * G_{\sigma_i}$ of multiscale markers obtained from sampling a Gaussian scale-space, where G_σ denotes an isotropic 2D Gaussian function of standard deviation σ . As shown in Figure 1, the image edges and boundaries which have been blurred and shifted by the Gaussian scale-space are better preserved across scales by the multiscale levelings. The corresponding residuals texture components $r_i = f - u_i$ contain a hierarchy of multiscale texture components, whose extraction will be detailed in the following sections.

As an alternative to the linear scale-space marker selection, one can consider the use of anisotropic diffusion [13]. At each sequence step the

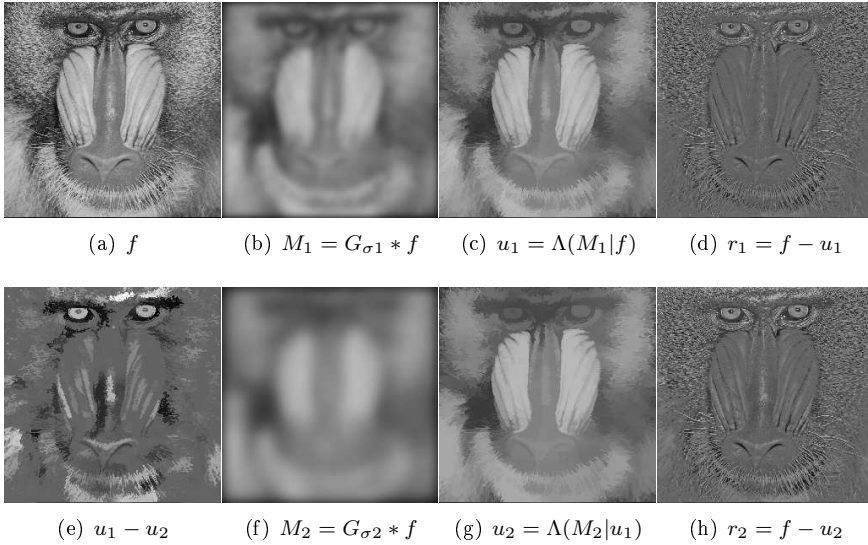


Figure 1. Multiscale leveling cartoons and $u + v$ decomposition. (a) Reference f . (b) Gaus. Marker 1 ($\sigma_1 = 4$). (c) Leveling 1 (u_1). (d) Residual 1 ($r_1 + 100$). (e) Levelings difference $u_1 - u_2$. (f) Gaus. Marker 2 ($\sigma_2 = 8$). (g) Leveling 2 (u_2). (h) Residual 2 ($r_2 + 100$).

leveling marker is obtained by a version of the image with blurred regions but adequately preserved boundaries, caused by the constrained diffusion process. Levelings obtained using anisotropic diffusion markers tend to retain information about edges in smaller scales on the cartoon component.

Proposition 1. *Levelings decrease the TV norm:*

(a) *If $u = \Lambda(M|f)$, then $\iint \|\nabla u\| \leq \iint \|\nabla f\|$.*

(b) *If $u_i = \Lambda(M_i|u_{i-1})$ with $u_0 = f$, then for all i*

$$\iint \|\nabla u_{i+1}\| \leq \iint \|\nabla u_i\| \leq \iint \|\nabla f\|. \quad (17)$$

Proof. (a) The levelings create flat plateaus on which the gradient becomes zero. The remaining slopes are the same as for the function. (b) results from (a). \square

We can compare our proposed leveling cartoons with the ones derived as the solutions of the TV minimization problem (2) along several directions: (i) The levelings preserve the regional maxima and minima and do not create new ones, while the TV cartoons preserve the global mean value. (ii) The levelings couple and preserve the sense of variation between neighbor pixels (14) whereas the TV cartoons preserve the global variance. (iii) By

Proposition 1, the levelings are related to a TV minimization. Further, the TV norm of the leveling cartoon decreases monotonically if we use a hierarchy of multiscale levelings. (iv) The presence of the marker image M gives a leveling cartoon far greater flexibility and multiscale capabilities than the simple regularization constants which control the scale of the TV cartoon.

4. Texture modulation energy

4.1 AM-FM Texture model and energy

Locally narrowband image textures can be modeled as 2D spatial AM-FM signals

$$f(x, y) = a(x, y) \cos[\phi(x, y)], \quad \vec{\omega}(x, y) = \nabla\phi(x, y), \quad (18)$$

that are 2D nonstationary sines with a spatially varying amplitude $a(x, y)$ and a spatially-varying instantaneous frequency vector $\vec{\omega}(x, y)$. In particular, the amplitude is used to model local image contrast and the frequency vector contains rich information about the locally emergent spatial frequencies. Thus, it is reasonable to assume that the amplitude $a(x, y)$ and frequency vector $\vec{\omega}(x, y)$ are locally narrowband signals and hence locally smooth. Such modulation models have been proposed by Bovik et al. [2] and Havlicek et al. [4] and have been applied to a variety of image processing and vision problems.

An important problem in modeling image textures with spatial AM-FM signals is to estimate the 2D amplitude and frequency signals using computational vision algorithms that have low complexity and small estimation error. Such an efficient approach was developed in [5] based on an energy operator $\Psi(f) \triangleq \|\nabla f\|^2 - f\nabla^2 f$, which is a multidimensional extension of the 1D Teager energy operator. Applying Ψ to a 2D AM-FM signal $f(x, y) = a(x, y) \cos[\phi(x, y)]$ modeling a texture component yields

$$\Psi[a \cos(\phi)] \approx a^2 \|\vec{\omega}\|^2, \quad (19)$$

which equals the product of the instantaneous amplitude and frequency magnitude squared and may be called the *texture modulation energy*. The above approximation error is negligible assuming that the instantaneous amplitude and frequency do not vary too fast in space or too greatly in value compared with the carriers. Further, if we also apply the energy operator on the image derivatives $\partial f/\partial x$ and $\partial f/\partial y$, then it is possible to separate the energy into its amplitude and frequency components via a nonlinear algorithm called Energy Separation Algorithm (ESA) [5].

4.2 Multiband texture energy tracking

In Bovik et al. [2] the AM-FM models are not applied directly to the whole (possibly wideband) image. Instead they are used on its bandpass filtered

versions that are outputs from a filterbank consisting of 2D Gabor filters. Bandpass filtering isolates highly active texture modulations and has some useful consequences like an increased noise tolerance and the enforcement of some smoothness on the amplitude and frequency signals. The motivation in using Gabor filters is their inherent property to be smooth, compact and attain the lower limit of joint space-frequency resolution uncertainty and model early filtering stages of human vision. The concept of using multiple frequency bands from a bank of bandpass filters for purposes of texture analysis or segmentation has been used with success in previous works, e.g. [2, 4, 5].

The oscillating functions, indicated by Meyer [10] to model and extract the v component, can be sought via AM-FM image modeling that reveals modulations and the existence of contrast and spatial frequency oscillations. Motivated by the analogies between the modulation models and Meyer’s indications we aim to capture oscillatory textural energy by a modified energy operator, through a multiband filtering-modulation based process.

In our work the extracted textured part is filtered through a bank of 2D Gabor filters, which are characterized by impulse response of the form $h_k(x, y) = e^{-\alpha^2 x^2 - \beta^2 y^2} \cos(\Omega_{k1}x + \Omega_{k2}y)$, where $\alpha/2\pi, \beta/2\pi$ are the rms bandwidths in each dimension and $(\Omega_{k1}, \Omega_{k2})$ is the k -th filter’s central frequency pair. The filters are uniformly arranged in the spatial frequency domain, in a polar wavelet-like tessellation, with equal and directional symmetric bandwidths and cover densely the frequency domain.

The filtered texture components from each filter output are then averaged by a local averaging filter h_a and the 2D Energy Operator Ψ is applied. We keep the value of the filter with the *Maximum Average Teager (MAT) Energy* per pixel, given by

$$\Psi_{\text{mat}}(v(x, y)) = \arg \max_k \Psi[(v * h_k) * h_a](x, y)$$

(* denotes convolution), as a means of tracking the most active texture component. The derived Ψ_{mat} is a slowly-varying indication of texture modulation energy, which can classify among different energy levels. It provides both local and global texture information and applied to the level-free v component, $\Psi_{\text{mat}}(v)$ is tracking the most active texture components along multiple modulation bands. Efficient discrete schemes exist for the numerical implementation of the 2D energy operator [3, 5].

The above ideas for texture modeling have been used for geometric active contour-based texture segmentation in Evangelopoulos et al [3]. In addition, the $u+v$ image decomposition using levelings for u and texture energy from v was used in a coupled watershed plus texture PDE-based segmentation scheme [15].

In Figure 2 we explore the efficacy of finding dominant components via the MAT Energy for detecting texture areas. This procedure can provide us with *texture energy markers*. We observe that the square root of MAT

energy (or even better its higher roots) successfully mark texture areas. Further, notice the lack of image structure and structure features (e.g. edges, blobs) in the markers extracted from the leveling residual r_1 .

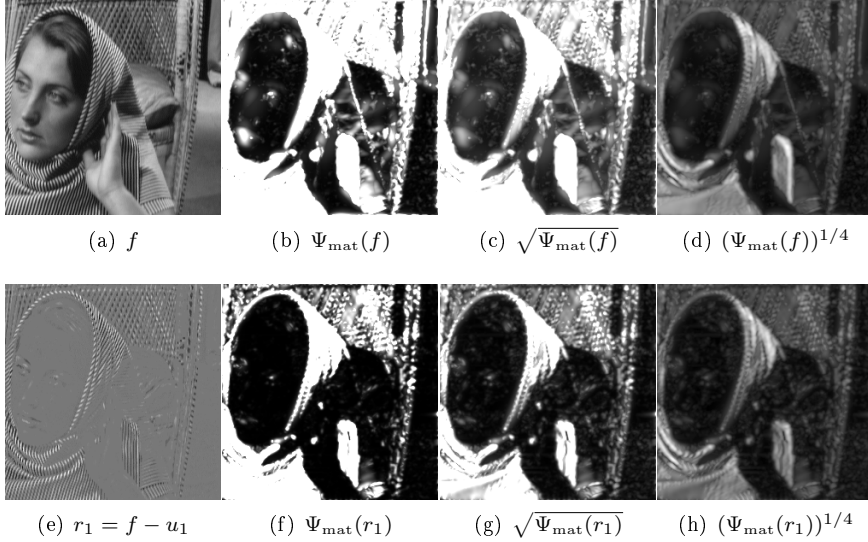


Figure 2. Texture energy markers and texture detection. Application of the Ψ_{mat} operator and its variants on initial f and the first leveling residual $r_1 = f - u_1$, where $u_1 = \Lambda(f * G_{\sigma_1}|f)$ with $\sigma_1 = 2$. For display, images in (b),(c) and (f),(g) are shown by upper thresholding the energy range at its average value and then linearly stretching onto $[0,1]$.

5. Experiments on image decomposition

Motivated by the ability of the levelings to yield the cartoon component u , either at the first or at the second marker scale, we experimentally investigate in this section two possible schemes to extract the texture component v from the residual r between the image and its leveling.

The first approach uses Gaussian markers both on the original image f to yield the cartoon u (at second scale) as well as on the first residual to yield the texture component according to the algorithm

$$\begin{aligned}
 u_1 &= \Lambda(M_1|f), & M_1 &= f * G_{\sigma_1}, \\
 u &= u_2 = \Lambda(M_2|u_1), & M_2 &= f * G_{\sigma_2}, \\
 r_1 &= f - u_1, \\
 u_r &= \Lambda(M_3|r_1), & M_3 &= r_1 * G_{\sigma_3}, \quad \sigma_3 = \sigma_1/2, \\
 v &= r_1 - u_r.
 \end{aligned} \tag{20}$$

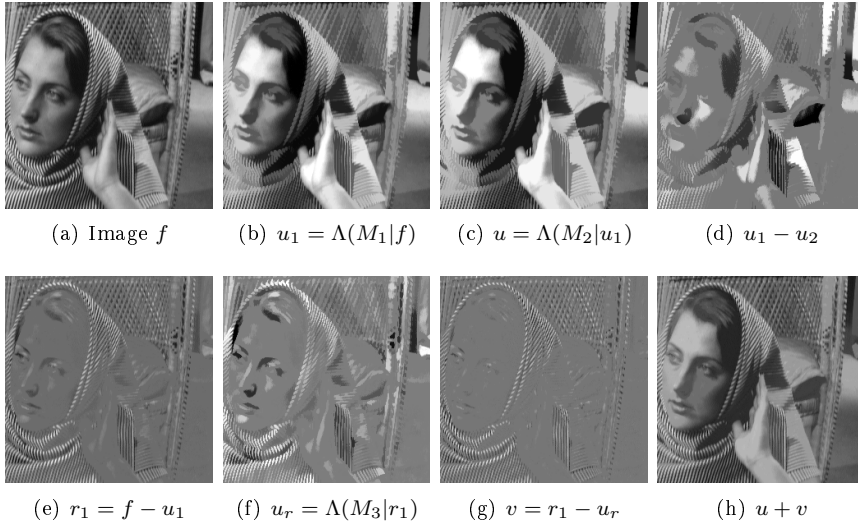


Figure 3. Multiscale leveling cartoon and $u + v$ decomposition. Top row: (a) Image f , (b) Leveling 1 (u_1) with Gauss marker $f * G_{\sigma_1}$ ($\sigma_1 = 5$), (c) Cartoon/Leveling 2 (u_2) with ($\sigma_2 = 10$), (d) Leveling difference ($u_2 - u_1$). Bottom row: (e) Residual $r_1 = f_1 - u_1$, (f) Leveling of r_1 with Gauss marker ($\sigma_3 = \sigma_1/2$), (g) Texture / residual ($v = r_1 - u_r$), (h) Reconstruction ($u + v$).

Figure 3 shows the results of the above algorithm. Figure 4 compares them with the Vese-Osher approach. In this comparison, we note the following.

- (i) Decompositions may not be comparable, are not optimum, only made with same L_2 norms on estimated v . (This equality of norms on the two texture components was enforced for purposes of comparison).
- (ii) Leveling u_Λ is sharper, yields clearer figure and large scale boundaries, u_{VO} is somehow smoother with smeared less-sharp edges.
- (iii) The previous advantage of the leveling cartoon has a tradeoff with the structure kept and evident in w_Λ .
- (iv) Smaller-scale structural details (e.g., facial characteristics) are preserved in u_Λ .
- (v) Texture components seem similar.
- (vi) More texture remains in w_{VO} than on w_Λ , though the latter has kept more structure.
- (vii) The reconstruction $u_\Lambda + v_\Lambda$ from levelings tends to ‘quantize’ the intensity values.

- (viii) What kind of residual is this ‘noise’ w_{VO} ? Is it really modeling image noise or something else? There is actually a mathematic formula for it, since three levelings are required in total to produce it:

$$w_{\Lambda} = f - u - v = \Lambda(M_1|f) - \Lambda[M_2|\Lambda(M_1|f)] + \Lambda[M_3|f - \Lambda(M_1|f)]. \quad (21)$$

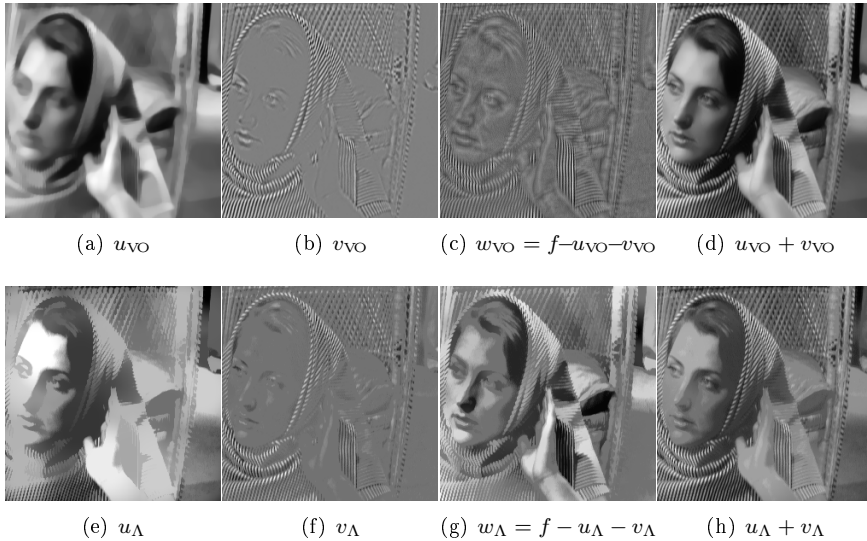


Figure 4. Comparisons with Vese-Osher $u + v$, left to right cartoon u , texture v , residual noise $w = f - u - v$ and image reconstruction from the model $u + v$. Top row: Vese-Osher algorithm with parameters $(\lambda_{\text{VO}}, \mu_{\text{VO}}) = (5, 0.1)$. Bottom row: Leveling decomposition with Gaussian markers $(\sigma_1, \sigma_2) = (10, 16)$. Parameters for both schemes were chosen so that the texture components have almost equal L_2 norms, i.e. $\|v_{\text{VO}}\|_2 = \|v_{\Lambda}\|_2$. All image values are stretched at full grayscale for display

Next we propose an alternative approach that uses the same algorithm for the cartoon u but derives the texture v by applying a leveling on the cartoon residual based on some type of texture energy markers:

$$v = r_1 - \Lambda(\pm\Psi_{\text{mat}}(r_1)|r_1). \quad (22)$$

Figure 5 shows several choices for such energy markers. In our experiments, the best results visually were achieved by using as marker a signed version of the MAT energy of the residual (or possibly its square root). This can be observed both in the resulting texture image component v and its profiles (no slow variation is left on v and the result seems zero-mean).

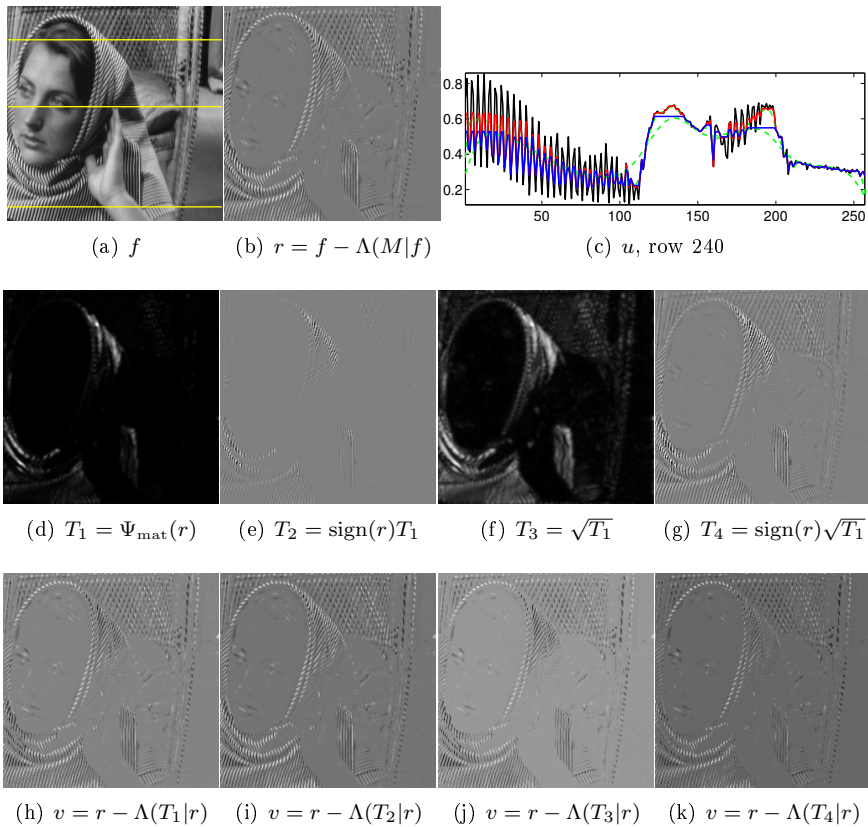


Figure 5. Markers T based on texture energy and leveling $\Lambda(T|r)$ of cartoon residual $r = f - \Lambda(M|f)$, where $M = f * G_\sigma$. Top row: image f , cartoon residual r and profile of row 240 (black: f , red: r , blue: u , green: marker). Middle row: Texture markers extracted from residual. Bottom row: Final texture components.

6. Conclusions

For the purpose of $u + v$ image decomposition, we have proposed hierarchical levelings based on Gaussian scale-space markers as a candidate model for image cartoons u . This was theoretically and experimentally supported. Further, we provided a viable approach to extract the texture part v based on levelings of the cartoon residuals. An improved version of the texture estimation resulted by performing energy-based dominant component analysis among multiple frequency bands and using this to create as texture detection markers for the levelings of the residuals.

There are numerous applications of the above ideas and algorithms. An ongoing research involves the restoration of ancient wallpaintings from

cracks and missing parts by performing the previous $u + v$ decomposition, from which the resulting u part achieves a significant degree of inpainting of the wide cracks and holes in these images, whereas the texture part contains the thin crack lines to be exploited by some further processing. An example of this application is illustrated in Figure 6. There we see that the leveling-based cartoon u is sharper and its corresponding texture v (based on energy markers) contains less structure than previous approaches.

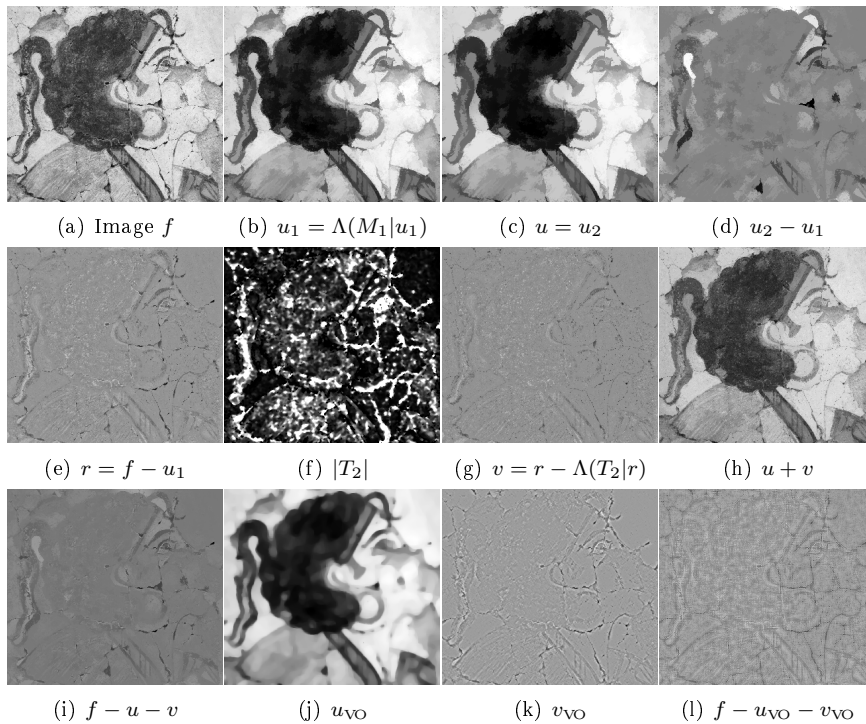


Figure 6. Leveling $u + v$ decomposition for image restoration. Top row: (a) Image f , 300×330 pixels from (6:1) subsampled “Potnia” wallpainting (*prehistoric Thira Acrotiri*), (b) Leveling 1 (u_1) with marker $f * G_\sigma$, where G_σ Gaussian ($\sigma_1 = 4$), (c) Cartoon/ Leveling 2 (u_2), with ($\sigma_2 = 8$), (d) Residual of levelings ($u_2 - u_1$). Middle row: (e) Residual $r = f - u_1$, (f) Texture energy ($T = \Psi_{\text{mat}}(r)$) used for marker $T_2 = \text{sign}(r)\sqrt{T}$, (g) Texture ($v = r - \Lambda(T_2|r)$), (h) Reconstruction ($v + u$), (i) Modeling error/fidelity, (j),(k),(l) Vese-Osher ($u_{\text{VO}}, v_{\text{VO}}$) and fidelity ($f - u_{\text{VO}} - v_{\text{VO}}$) with $(\lambda_{\text{VO}}, \mu_{\text{VO}}) = (5, 0.1)$.

Acknowledgments

This work was supported by the European Network of Excellence MUSCLE and by grants IIENEΔ-2003 EΔ865 and IIENEΔ-2001 [co-financed by E.U.-European Social Fund (75%) and the Greek Ministry of Development-GSRT (25%)]. We thank G. Papandreou and S. Lefkimmiatis for help with pdfLaTeX.

References

- [1] M. Bertalmio, L. Vese, G. Sapiro, and S. Osher, *Image filling-ing in a decomposition space*, Intl. Conf. on Image Processing, November 2003.
- [2] A. C. Bovik, N. Gopal, T. Emmoth, and A. Restrepo, *Localized measurement of emergent image frequencies by Gabor wavelets*, IEEE Trans. Inform. Theory **38** (March 1992), no. 3, 691–712.
- [3] G. Evangelopoulos, I. Kokkinos, and P. Maragos, *Advances in Variational Image Segmentation Using AM-FM Models: Regularized Demodulation and Probabilistic Cue Integration*, Proc. VLSM 2005: Springer LNCS 3275, 2005, pp. 121–136.
- [4] J. P. Havlicek, D. S. Harding, and A. C. Bovik, *Multidimensional quasi-eigenfunction approximations and multicomponent AM-FM models*, IEEE Trans. Image Proc. **9** (February 2000), no. 2, 227–242.
- [5] P. Maragos and A. C. Bovik, *Image Demodulation using Multidimensional Energy Separation*, J. Opt. Soc. Amer. A **12** (September 1995), no. 9, 1867–1876.
- [6] P. Maragos, *Algebraic and PDE Approaches for Lattice Scale-Spaces with Global Constraints*, Int'l J. Computer Vision **52** (2003), no. 2-3, 121–137.
- [7] ———, *A Variational Formulation of PDEs for Dilations and Levelings*, Proc. Int'l Symp. Math. Morphology (ISMM 2005), 2005.
- [8] F. Meyer, *The Levelings*, Proc. 4th Int'l Symp. Math. Morphology and its Applications to image processing, June 1998, pp. 199–206.
- [9] F. Meyer and P. Maragos, *Nonlinear Scale-Space Representation with Morphological Levelings*, J. Visual Communication and Image Representation **11** (June 2000), no. 2, 245–265.
- [10] Y. Meyer, *Oscillating Patterns in Image Processing and Nonlinear Evolution Equations*, University Lecture Series, vol. 22, AMS, 2001.
- [11] J. M. Morel and S. Solimini, *Variational Methods in Image Segmentation*, Birkhauser, Boston, 1995.
- [12] D. Mumford and J. Shah, *Optimal Approximations by Piecewise Smooth Functions and Associated Variational Problems*, Communic. Pure and Applied Math. **42** (1989), no. 5, 577–685.
- [13] P. Perona and J. Malik, *Scale-Space and Edge Detection Using Anisotropic Diffusion*, IEEE Trans. Pattern Anal. Mach. Intell. **12** (1990), no. 7, 629–639.
- [14] L. Rudin, S. Osher, and E. Fatemi, *Nonlinear Total Variation based Noise Removal Algorithms*, Physica D: Nonlinear Phenomena **60** (1992), no. 1-4, 259–268.
- [15] A. Sofou, G. Evangelopoulos, and P. Maragos, *Coupled Geometric and Texture PDE-based Segmentation*, Proc. Int'l Conf. Image Processing, 2005, pp. II–650–3.
- [16] L. A. Vese and S. J. Osher, *Modeling textures with total variation minimization and oscillating patterns in image processing*, SIAM J. Scientific Computing **19** (2003), no. 1-3, 553–572.
- [17] ———, *Image Denoising and Decomposition with Total Variation Minimization and Oscillatory Functions*, J. Math. Imaging and Vision **20** (2004), 7–18.